

SOURCE: A Semi-automatic Tool for Spring Monitoring Data Analysis and Aquifer Characterization

Stefano Lo Russo

Politecnico di Torino

Enrico Suozzi

Politecnico di Torino

Martina Gizzi (✉ martina.gizzi@polito.it)

Politecnico di Torino <https://orcid.org/0000-0001-7791-3260>

Glenda Taddia

Politecnico di Torino

Research Article

Keywords: Mountain Springs, Hydrogeology, Hydrology, Python App, Spring Vulnerability

Posted Date: March 10th, 2021

DOI: <https://doi.org/10.21203/rs.3.rs-227065/v1>

License:  This work is licensed under a Creative Commons Attribution 4.0 International License.

[Read Full License](#)

27 **1. Introduction**

28 Mountain aquifers represent one of the largest and most valuable sources of water in northern Italy and are
29 necessary to meet the water needs of the population. In recent decades, different hydrological issues, such as
30 the gradual drying up of many springs, low discharge rates during dry months, and formerly perennial springs
31 becoming seasonal, have been reported in studies from throughout the Italian Alps and Apennines (Cambi and
32 Dragoni 2000; Fiorillo et al. 2007; Gattinoni and Francani 2010). Additionally, because mountain springs are
33 fed by shallow groundwater resources, they are often highly vulnerable to contamination (Christie et al. 2013;
34 Amanzio et al. 2015).

35 Optimizing the current and future management of mountain groundwater resources and understanding their
36 recharging systems from a hydrogeological perspective is necessary for developing adequate resource
37 management strategies. In addition, groundwater resources must be correctly quantified to provide information
38 for the assessment of the effects of climate change on water resources (Middelkoop et al. 2001; Tague et al.
39 2012). In this context, new automated techniques and tools need to be applied to the estimation of aquifer
40 hydrogeological parameters in order to fully understand the dynamics of exhausting available groundwater
41 resources.

42 Over decades, a large number of methodologies have been developed to derive hydrogeological information
43 about mountain spring recharging systems. Known methods for analysing hydrograph recession periods are
44 based on the Boussinesq and Maillet equations (Boussinesq 1904; Maillet 1905). The Boussinesq equation is
45 used to determine hydrogeological parameters, while the Maillet exponential formula generates good fits for
46 hydrograph recession curves and accurately describes recession phenomena over long periods (Kovács et al.
47 2005); any deviation from the exponential trend may indicate the presence of hydraulic anisotropies (Amit et
48 al. 2002; Fiorillo 2014). However, in some cases, the exponential method was found to overestimate the period
49 of the influenced regime and underestimate the dynamic volume of the aquifer (Dewandel et al. 2003).

50 Various recent studies have expanded autocorrelation and cross-correlation methods and applied them to
51 mountain spring monitoring datasets. In particular, the univariate (autocorrelation) method has been used to
52 analyse the characteristics and structure of individual time series; the bivariate (cross-correlation) method has
53 been used to investigate the connection between input and output time series (Amanzio et al. 2015; Lo Russo
54 et al. 2018). Several applications of auto- and cross-correlation methods examining the relation between

55 rainfall and daily spring discharge are available in the literature on karst spring environments (Angelini 1997;
56 Larocque et al. 1998; Panagopoulos and Lambrakis 2006).

57 Fiorillo and Doglioni (2010), Lo Russo et al. (2015) and Banzato et al. (2017) have recently demonstrated how
58 aquifer drainage models and mountain spring vulnerability can be evaluated by analysing continuous
59 measurements of discharge (Q), precipitation (P), temperature (T) and electrical conductivity (EC). Different
60 methods have been proposed to assess the vulnerability level of an aquifer (Gogu and Dassargues 2000). As
61 springs are usually located in mountainous zones, the use of parametric methods such as SINTACS (Civita
62 and De Maio 1997), DRASTIC (Aller et al. 1987) or GOD (Foster 1987) is often impossible; these methods
63 are primarily based on hydrostratigraphic information usually unavailable in mountainous areas since core
64 drillings are somewhat rare in such locations. However, spring monitoring datasets continuously recorded by
65 multiparametric probes are usually available; these data can be used to properly analyse groundwater
66 vulnerability in mountain areas. Utilizing monitored parameters, Galleani et al. (2011) proposed a new
67 analytical approach called the VESPA (Vulnerability Estimator for Spring Protection Areas) index, which is a
68 useful methodological tool to assess the behaviour of mountain spring drainage systems through analysing
69 spring responses to different recharge impulses.

70 Because the analytical examination of individual recession periods can generate inconsistencies related to the
71 complexity of groundwater circulation, analysing the recorded values for mountain springs by comparing
72 different recession periods and applying different methodologies is essential for properly characterizing
73 recharge systems (Gizzi et al. 2020). To do this, data processing times must be shortened; researchers and
74 applied hydrogeologists must develop new automated techniques and tools to apply in mountain aquifer
75 analysis.

76 Different types of automated calculation codes have been developed to properly analyse spring hydrographs.
77 The RC software developed by the Hydro Office of the Department of Hydrogeology of Comenius University
78 in Bratislava (in collaboration with the Department of Hydrogeology and Geothermal Energy of the Geological
79 Survey of Slovak Republic) and the USGS GW Toolbox (Barlow et al. 2017) are two well-known examples.
80 However, these software do not allow for estimation of the vulnerability index using methods such as VESPA,
81 and they do not apply autocorrelation and cross-correlation functions to analyse recorded signals.

82 This paper introduces SOURCE (a semi-automatic tool for Spring mOnitoring data analysis and aqUifeR
83 CharactErization), a program that automates the hydrogeological characterisation of spring aquifers. Input data
84 (flow rate, temperature, hydraulic conductivity and rainfall) for particular time intervals can be selected and
85 uploaded in a formatted Excel file. The data can be processed, providing graphical outputs and values for the
86 main hydrodynamic parameters of the analysed aquifer.

87 The main functionalities of this tool are presented through a case study of the Mascognaz mountain springs
88 (Aosta Valley, north-western Italy).

89 The beta version of this software has been developed within the framework of the INTERREG ITALY-
90 SWITZERLAND RESERVAQUA project, which aims to quantify and identify water reserves in order to
91 protect cross-border mountain water springs like the Mascognaz springs.

92 **2. Methods**

93 **2.1 Case study: The Mascognaz springs**

94 The Mascognaz springs are one of the most important test sites in the Aosta Valley mountain sector. Over the
95 last decade, several projects by researchers from Politecnico di Torino have installed sophisticated instruments,
96 such as multiparametric water probes, different types of sensors and a meteorological station, to continuously
97 monitor the two Mascognaz springs and collect information on their recharging systems. This equipment and
98 the data it has continuously gathered are readily available to researchers, allowing them to accurately study
99 how climate change influences aquifer recharge in a mountain basin not fed by a glacier. In addition, trend
100 data for the Mascognaz springs can be compared to meteorological trend data for the valley.

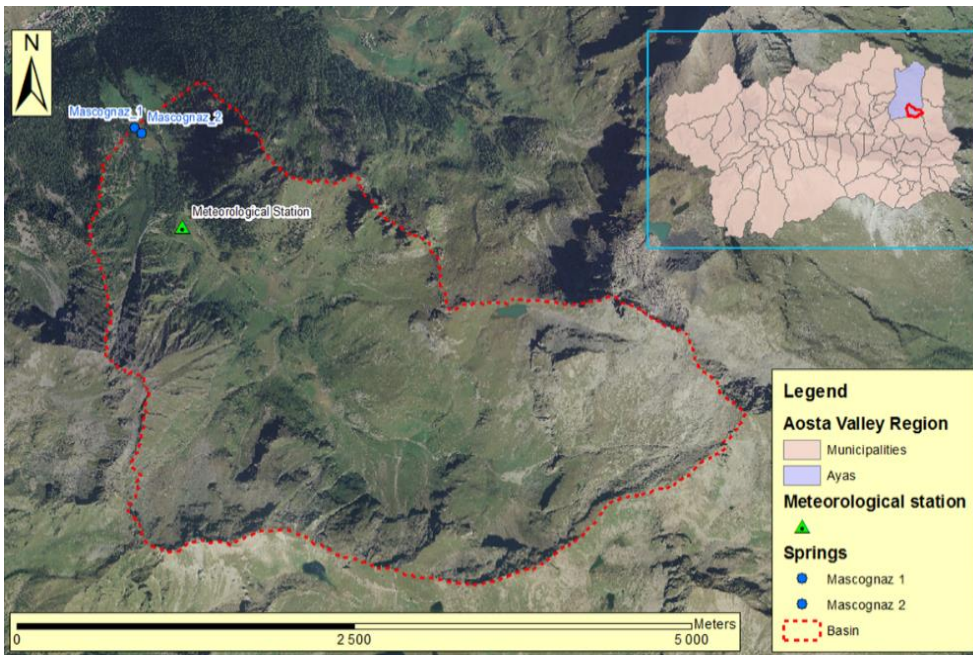


Figure 1: Mascognaz springs location

101 Both Mascognaz springs (Mascognaz 1 and Mascognaz 2) are located inside the Mascognaz Valley (Ayas
 102 Municipality, Aosta Valley), at an elevation of 1870 m above sea level (Fig. 1). The Mascognaz Valley has a
 103 typical alpine climate, with cold winters and cool summers. Autumn has the highest monthly rainfall, with
 104 approximately 110 mm per month. Summer has the lowest monthly rainfall, with a mean of about 30 mm per
 105 month.

106 The Mascognaz springs are located within the Combin geological complex, which belongs to the Piedmont
 107 Zone geological sequence and consists of metabasalts and subordinate Mesozoic metasediments representative
 108 of the local impermeable bedrock (Dal Piaz 1992). Overlaying Quaternary cover sheets consist mostly of
 109 glacial and landslide deposits of variable thickness. A highly permeable shallow aquifer supplies the
 110 Mascognaz springs. The Quaternary deposits over the Mascognaz springs catchment area (10 km²) have a
 111 maximum estimated depth of 20 m.

112 Due to the suitable monitoring datasets provided by the multiparameter probes and meteorological station, the
 113 Mascognaz springs were selected as an ideal case study for this study (Fig. 2). Extensive information on the
 114 local hydrogeological setting and the catchment area, which indicated that the groundwater divide and

115 watershed boundaries coincide, is useful for properly understanding and characterizing the results obtained
116 from the water-spring analysis.



Figure 2: Overview of the instruments installed in the Mascognaz 1 spring

117 2.2 Spring recession curve analysis

118 Analysing spring discharge hydrographs is one of the most useful tools when studying mountain springs and
119 defining aquifer characteristics, such as the type and quantity of its groundwater reserves.

120 There have been several studies on recession curve modelling, each establishing different mathematical
121 relationships between the water spring discharge parameter (Q) and recording time (t). Boussinesq (1904) and
122 Maillet (1905) proposed two different analytical formulas that describe the dependence of the flow rate at a
123 specified time (Q_t) on the flow rate at the beginning of the recession (Q_0). These formulas allow for the
124 calculation of the available water volume at different moments in time. Boussinesq developed an exact
125 analytical solution of the diffusion equation that describes flow through a porous medium by assuming a
126 porous, free, homogeneous and isotropic aquifer limited by an impermeable horizontal layer at the level of the
127 outlet:

$$Q_t = \frac{Q_0}{(1 + \alpha(t - t_0))^2} \quad (1)$$

128 where Q_t (m^3/s) is the flow rate value at $t \neq t_0$, Q_0 is the flow rate at $t = t_0$ and α is the recession coefficient, a
129 constant that depends only on the aquifer hydraulic systems, as shown below.

$$\alpha = \frac{\sqrt{Q_0} - \sqrt{Q_t}}{\sqrt{Q_t t}} \quad (2)$$

130 Maillet showed that the recession of a spring can be represented by an exponential formula, implying a linear
131 relationship between the hydraulic head and flow rate:

$$Q_t = Q_0 e^{-\alpha(t-t_0)} \quad (3)$$

132 where the recession coefficient α can be determined using the following equation.

$$\alpha = \frac{\log Q_0 - \log Q_t}{e^{(t-t_0)}} \quad (4)$$

133 In both methods, the recession coefficient equations are used to determine important hydrogeological
134 parameters: W_0 , the groundwater volume stored above spring level at the end of the recharging season
135 (beginning of the recession; Eq. 5 and 7), and W_d , the groundwater volume stored at the end recession period
136 (Eq. 6 and 8).

Boussinesq (1904)

$$W_0 = \frac{Q_0}{\alpha (1 + \alpha t)^2} \times 86400 \quad (5)$$

$$W_d = \left[\frac{Q_0}{\alpha} - \frac{Q_0}{\alpha(1 + \alpha t)} \right] \times 86400 \quad (6)$$

Maillet (1905)

$$W_0 = \frac{Q_0}{\alpha} \times 86400 \quad (7)$$

$$W_d = \frac{(Q_0 - Q_t)}{\alpha} \times 86400 \quad (8)$$

137 2.3 Autocorrelation and cross-correlation functions

138 The autocorrelation function (ACF) can evaluate the linear dependency of successive values of a single
139 parameter for a defined time series. The method is univariate and quantifies the memory effect that corresponds
140 to the temporal reciprocal influence on subsequent data of a single dataset.

141 Statistically, the autocorrelation of a random process describes the correlation between values of the process
142 at different points in time as a function of the two times or the time difference. The autocorrelation for a
143 distance τ corresponds to the covariance of all measurements x_t and measurements with a time distance $x_{t+\tau}$,
144 according to the following equation:

$$cov\tau = \frac{1}{n - \tau} \sum_{t=1+\tau}^n x_t x_{t-\tau} - X_t X_{t-\tau} \quad (9)$$

145 where x is a time series, n is the number of measurements in the time series, τ is the time distance between two
146 measurements, and X is the average value of the sample. The autocorrelation coefficient (ACC) ranges from -1
147 to 1. An ACC of 1 means that the compared time series are identical.

148 When using the ACF on hydrological data, a slow decline indicates an aquifer characterised by low draining
149 properties, low permeability or major groundwater storage. Conversely, a fast decline indicates a more rapid
150 flow of water through the aquifer and/or limited storage capacity (Imagawa et al. 2013; Reberski et al. 2013).

151 Traditionally, the ACC accounts for Q data, and the main hydrogeological assessment is obtained through such
152 an analysis. However, the ACC values can also be applied to T and EC, and these analyses can be used to
153 validate the hydrogeological view of the spring memory effect, which is based on Q data. The time-level
154 stabilities of T, EC and Q can be good markers of a high residence time in an aquifer (Lo Russo et al. 2015).

155 To identify any instances of pronounced similarity or linear correlation between individual data, two different
156 time series can be compared using the cross-correlation function (CCF; e.g., rainfall versus discharge
157 parameters). Cross-correlation analysis is based on an equation similar to the ACF. If two time series are
158 marked as variables X and Y , and n is the number of pairs that are compared in one step (k) of the CCF, the
159 cross-correlation coefficient can be obtained by the following (Box and Jenkins 1974):

$$R_{xy}(K) = \frac{n \sum XY - \sum X \sum Y}{\sqrt{[n \sum X^2 - (\sum X)^2] \times [n \sum Y^2 - (\sum Y)^2]}} \quad (10)$$

160 Values of $R_{xy}(K)$ can range between -1 (perfect negative correlation) and +1 (perfect positive correlation); a
161 value of 0 indicates no correlation.

162 As with the ACC, the CCF is an established technique that is usually applied on Q and P datasets. However,
163 the CCF can also assess T and EC datasets, and such analyses could be used to validate hydrogeological
164 considerations of the time lag response and maximum $R_{xy}(K)$ values.

165 Furthermore, the pollution vulnerability index of different springs can be estimated using the lag time derived
166 from cross-correlation analysis. This statistical method can be applied to explore the relation between discharge
167 and rainfall, as well as the relation between electrical conductivity and rainfall.

168 **2.4 VESPA index**

169 Properly identifying the vulnerability level of a mountain aquifer and its associated springs is necessary to
170 protect aquifers from potential pollution sources and preserve water quality over time.

171 Aquifers are fed by rainfall, snowmelt and surface runoff, collectively known as neo-infiltration water. Water
172 from these sources infiltrates the ground and becomes part of the underground flow. Because neo-infiltration
173 water can transport pollutants into groundwater systems, the rate at which neo-infiltration water enters
174 groundwater systems and its velocity toward a spring must be accurately evaluated.

175 Galleani et al. (2011) combined monitored hydrogeological parameters and proposed a new analytical
176 approach called the VESPA (Vulnerability Estimator for Spring Protection Areas) index, which assesses the
177 behaviour of springs drainage systems through an analysis of their responses to different recharge impulses.

178 The VESPA index V is defined using the following relationship (Banzato et al. 2017):

$$V = c(\rho)\beta\gamma \quad (11)$$

179 where $c(\rho)$ is the correlation factor. This factor is defined by the equation below.

$$c(\rho) = [\mu(-\rho) + \alpha\mu(\rho)]|\rho| \quad (12)$$

180 The ρ value represents the correlation coefficient between Q and EC , calculated using over 1 year of continuous
181 hourly data. The function $\mu(\rho)$ is the Heaviside step function:

$$u(\rho) = \{1 \ \rho \geq 0 ; 0 \ \rho < 0 \} \quad (13)$$

182 where α is the scaling coefficient, which can range from 0 and 1 but is generally assumed to be 0.5. The
183 variables β and γ are the temperature and discharge factors, respectively, and are defined by the following
184 equations:

$$\beta = \left\{ \frac{T_{max} - T_{min}}{1^\circ C} \right\}^2 \quad (14)$$

$$\gamma = \frac{Q_{max} - Q_{min}}{Q_{med}} \quad (15)$$

185 where T_{max} and T_{min} are the maximum and minimum temperatures, and Q_{max} , Q_{min} and Q_{med} are the maximum,
186 minimum and average discharge values for the monitoring period.

187 According to Eq. (11), spring vulnerability is strictly related to a change in one of the parameters (Q , T or EC).

188 The ρ correlation coefficient defines the aquifer behavioural category and identifies the type of response to the
 189 infiltrative input. From the value of the correlation coefficient ρ , drainage systems can be classified into one
 190 of three categories: highly effective (replacement effects prevail and $-1 \leq \rho \leq -0.2$); moderately effective
 191 (piston flow prevails and $0.2 \leq \rho \leq 1$); and weakly effective (the homogenisation phenomenon prevails and
 192 $-0.2 \leq \rho \leq 0.2$).

193 Based on the computed values of the VESPA index, a spring's vulnerability level can be defined according to
 194 the classification in Table 1 (Galleani et al. 2011).

VESPA Index Values and Their Vulnerability Levels		
$V \geq 10$	Very high	196
$1 < V < 10$	High	197
$0.1 < V < 1$	Medium	198
$0 < V < 0.1$	Low	199

Table 1: VESPA index values and their vulnerability levels (Galleani et al. 2011)

200 **3. Code**

201 The dynamics of mountain groundwater resource depletion are heavily influenced by climate conditions.
 202 Annual variations in snow and rain precipitation impact the hydrodynamic characteristics and exhaustion
 203 modalities of springs. As such, it is necessary to develop new automated techniques that will allow researchers
 204 to estimate the main parameters of mountain aquifers quickly and accurately. In order to propose a new,
 205 advanced, semi-automatic tool for spring characterisation that uses available parameter datasets, the above-
 206 described methodologies were implemented in Python.

207 Python is a high-level programming language with an object-oriented approach created by Guido van Rossum
 208 in 1991. The first version of this study's Python code was developed in 2014 at Politecnico di Torino within
 209 the framework of the Interreg Project between Italy and Switzerland. Over time, the tool was updated with the
 210 latest libraries of Python. In order to improve software performance, the number of libraries used has been
 211 limited, with preference given to common libraries over more experimental ones. In addition to the standard
 212 Python libraries, code for the proposed tool utilized the following:

- 213 • Numpy (<https://numpy.org/>), the fundamental package for scientific computing;

- 214 • Matplotlib (<https://matplotlib.org/>), a comprehensive library for creating static, animated and
 215 interactive visualisations; and
- 216 • Scipy (<https://www.scipy.org/>), a Python-based ecosystem of open-source software for mathematics,
 217 science and engineering.

218 The script of the final version of the code was connected to a Postgres Database, where all input information
 219 is stored. The final program can accept tabulated data in an Excel spreadsheet and is usable in virtual
 220 environments on Linux, Mac and Windows OS.

221 To be correctly input into SOURCE, Excel files must have a first sheet named "Spring_data" that contains the
 222 water spring data and a second sheet named "Meteo_data" that contains the meteorological data. With this
 223 format, it is possible to run the script and set parameters using the proposed GUI interface (Fig. 3). The
 224 following information is also required:

- 225 • **Filename:** the file path of the Excel document, type string;
- 226 • **Date start:** the start date for the data, type string;
- 227 • **Date stop:** the stop date for the data, type string;
- 228 • **Water spring name:** name of the spring to be analysed, type string;
- 229 • **Select type of analysis:** a choice of 'All', 'Recession curves', 'VESPA vulnerability index', 'Plot
 230 data' or 'Auto & Cross-correlation'; and
- 231 • **Select method for recession curves:** a choice of 'All', 'Maillet', 'Boussinesq' or 'none'.



Figure 3: GUI of the proposed Python tool

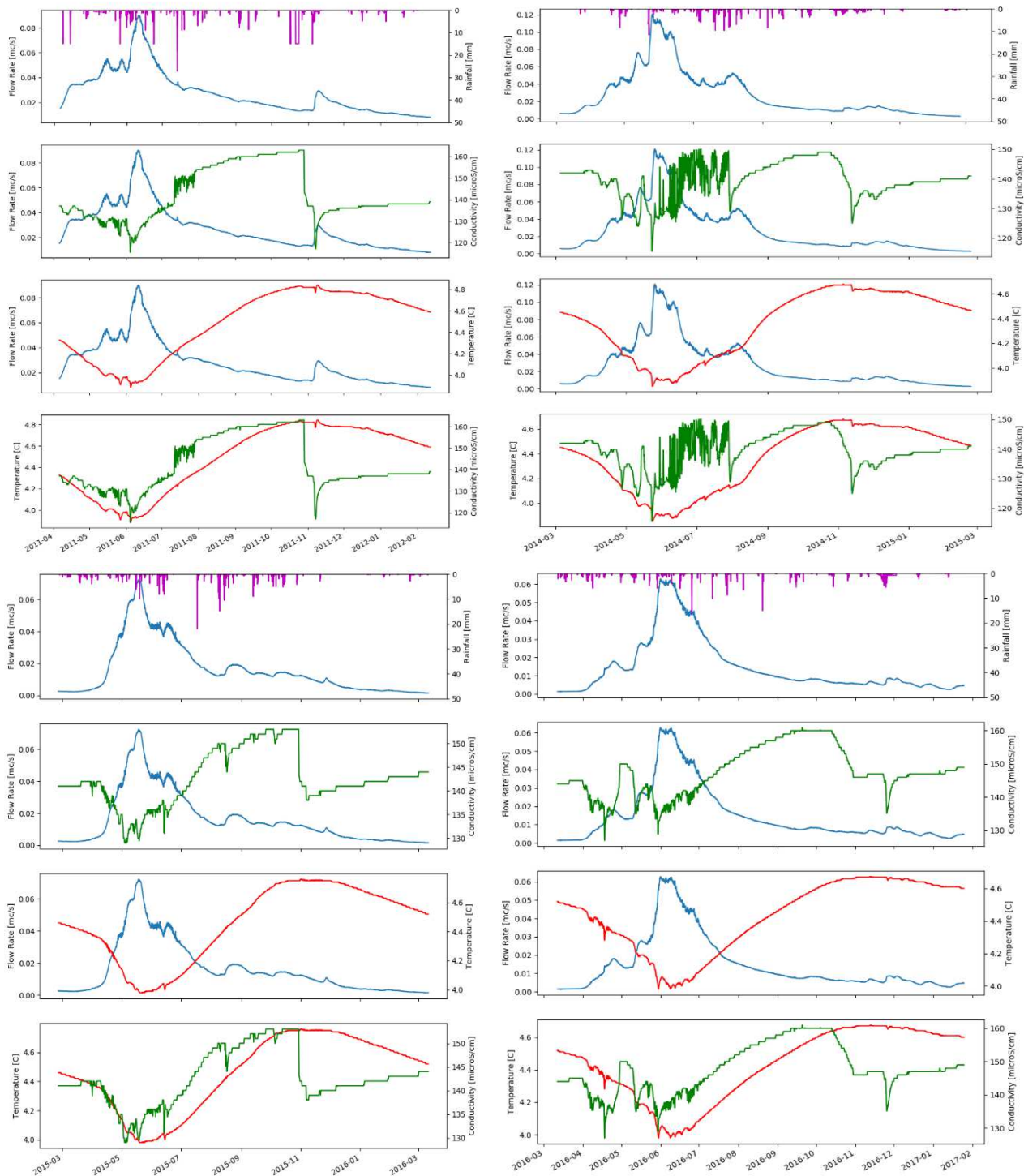
232 **4. Results**

233 Input data were recorded by the multiparametric probes installed in the Mascognaz 1 spring. Specific time
234 intervals were selected, and the data for this period were processed using the final version of the described
235 Python code. Graphical outputs and hydrodynamic parameter values for the analysed aquifer were obtained.
236 The monitoring datasets for the years 2012–2013, 2014–2015, 2015–2016 and 2016–2017 were selected for
237 analysis, and the outputs below were obtained and presented:

- 238 • Spring hydrographs
- 239 • Recession curves
- 240 • VESPA index
- 241 • Autocorrelation and cross-correlation coefficients

242 **4.1 Spring hydrograph**

243 The first graphical output that can be obtained are hydrographs for the spring under analysis. As reported in
244 Fig. 4, the Mascognaz 1 spring hydrographs were obtained by analysing data from the selected time range and
245 show variation in quick flow at the end of the winter period. Pronounced discharge fluctuations in the fast-
246 flow regime of the Mascognaz spring were due to contributions from snowmelt and the rapid infiltration of
247 precipitation during the autumn season. Abundant rainfall occurred during the autumn period of the selected
248 hydrographic years, causing the formation of a new peak and a decrease in the recorded values of T and EC.
249 Since the depletion curve was in approximately ideal conditions for each year analysed and was only weakly
250 influenced by infiltration events, the recession coefficients calculated using the Boussinesq (1904) and Maillet
251 (1905) methods can be considered reliable.



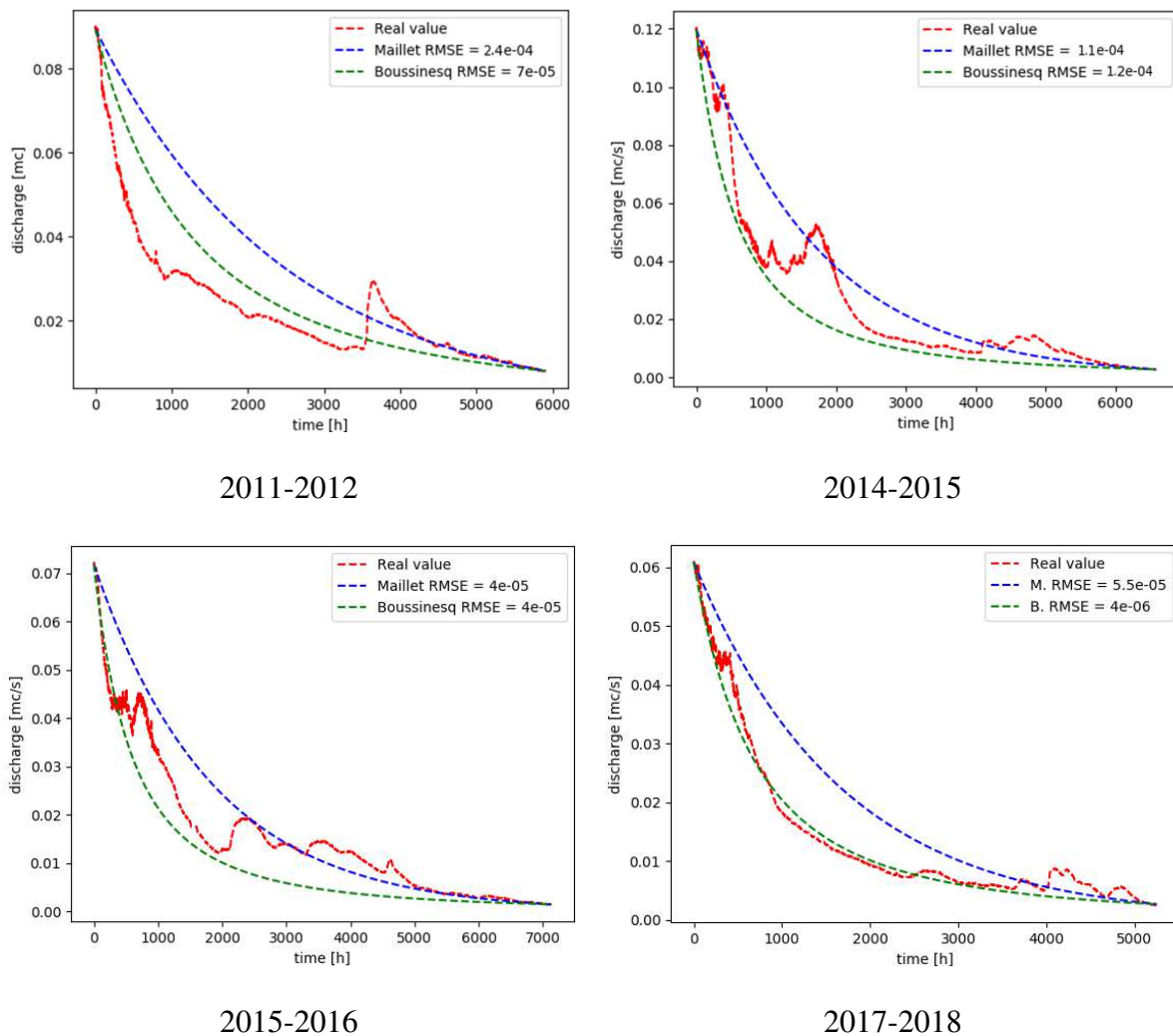
252 *Figure 4: Mascognaz 1 spring hydrographs (NW Start 2011-04-06, Stop 2012-02-12; NE Start 2014-03-05 Stop 2015-*
 253 *02-24; SW Start 2015-02-25 Stop 2016-03-11; SE Start 2016-03-12 Stop 2017-01-25) for rainfall (violet lines), flow*
 254 *rate (blue lines), electrical conductivity (green lines) temperature (red lines)*

255 **4.2 Recession curve**

256 The second possible graphical output is recession curves (Fig. 5). The aquifer parameters, calculated using the
 257 Boussinesq (1904) and Maillet (1905) methods, are reported in Tab. 3. The flow rate estimates from the

258 Boussinesq method closely matched the actual values reported for the years 2012–2013, 2015–2016 and 2017–
259 2018, but not for the year 2014–2015 (Fig. 5).

260 The duration of the exhaustion period, the time between snowmelt peaks and the annual minimum point before
261 the new recharge influence the α value. The minimum estimated value for α was 0.0094 (2011–2012,
262 Boussinesq) and the maximum value was 0.0206 (2014–2015, Boussinesq). The fluctuation depended mainly
263 on the amount of snow fall in winter (Tab. 2).



264 *Figure 5: Mascognaz 1 recession curves based on the Boussinesq (1904) and Maillet (1905) methods*

Parameter	2011–2012		2014–2015		2015–2016		2016–2017		Measure unit
	Maillet	Boussinesq	Maillet	Boussinesq	Maillet	Boussinesq	Maillet	Boussinesq	
Flow rate at the beginning of the recession (Q_0)	0.0895	0.0895	0.1198	0.1198	0.0719	0.0719	0.0608	0.0608	mc/s
Flow rate at the end of the recession (Q_i)	0.0081	0.0081	0.0027	0.0027	0.0015	0.0015	0.0026	0.0026	mc/s
Time $\neq t_0$	246	246	274	274	297	297	219	219	day
Recession coefficient	0.0098	0.0094	0.0138	0.0206	0.013	0.0200	0.0144	0.0174	-
Groundwater volume at the beginning of the recession (W_0)	792441	819580	749074	502850	476595	311160	366018	301313	mc
Groundwater volume at the end of the recession (W_d)	720543	572710	732074	427098	466666	266247	350266	238805	mc
Renewal rate	0.90927	0.69878	0.97731	0.84935	0.97917	0.85566	0.95696	0.79255	%
Renewal time rate (T_{rin})	1.1	1.431	1.023	1.177	1.021	1.169	1.045	1.262	years
Delay time	102.58	114.87	72.46	7.62	76.8	6.41	69.68	29.2	days
Depletion capacity	720504	739027.29	732059.82	501060.2	466657	310330.68	350254	294708.07	mc

265 *Table 2: Aquifer parameters calculated using the Boussinesq (1904) and Maillet (1905) methods*

266 **4.3 The VESPA index**

267 The third type of information that can be obtained from SOURCE is the value of the VESPA index. The
268 vulnerability index of the spring had a medium value for all the years analysed (Tab. 3). The obtained ρ
269 correlation coefficients for each year in the selected timeframe identify the spring as a weakly effective
270 drainage system where the homogenisation phenomenon prevails.

	2011	2014	2015	2016
rho	0.06	0.110	0.070	0.08
beta	0.94	0.690	0.610	0.49
gamma	3.08	5.040	3.970	3.91
VESPA index	0.176	0.370	0.162	0.153

Vulnerability	Medium	Medium	Medium	Medium
---------------	--------	--------	--------	--------

271 *Table 3: VESPA index values obtained for the Mascognaz 1 spring*

272 **4.4 Autocorrelation and cross-correlation coefficient**

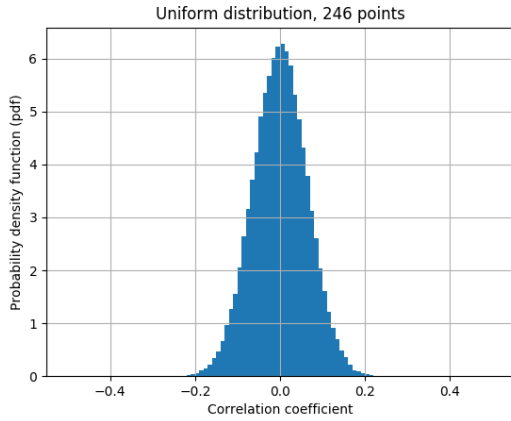


Figure 6: PDF of the estimated correlation coefficients (2011 dataset)

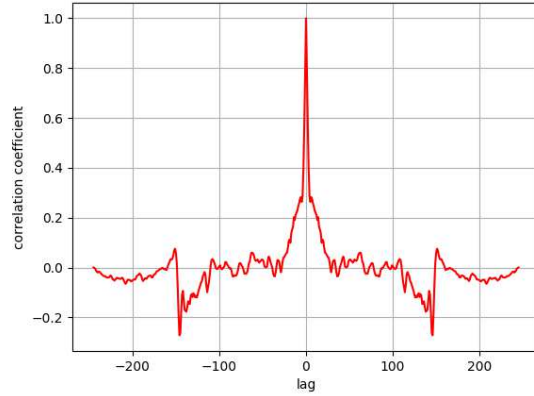


Figure 7: Estimated correlation coefficients, considering different time lags (2011 dataset)

273 The correlogram is a commonly used tool for checking the randomness of a dataset. If they are random,
 274 autocorrelations should be near zero for any time-lag separations considered. The correlation analysis was first
 275 performed on flow rate (Q) data. The distribution trend of the correlation coefficient reported in Fig. 6 can be
 276 identified as a Gaussian curve; the correlation coefficient values are concentrated in a narrow range of values,
 277 and so the maximum autocorrelation is obtained with a very short lag time (Fig.7).

	2011	2014	2015	2016
Correlation coefficient	0.107	0.2	0.15	0.11

278 *Table 4: Correlation coefficient values obtained for the Mascognaz spring 1, considering different analysed datasets*

279 As reported in Tab. 4, the correlation values tended to change over time. The Mascognaz springs
 280 autocorrelation lag varied within a narrow band across years, implying the series is not significantly correlated

281 with the delayed series; the variations from one instant or period to another are random phenomena (i.e., there
282 is an accidental component, or the stochastic part prevails; Fig. 8).

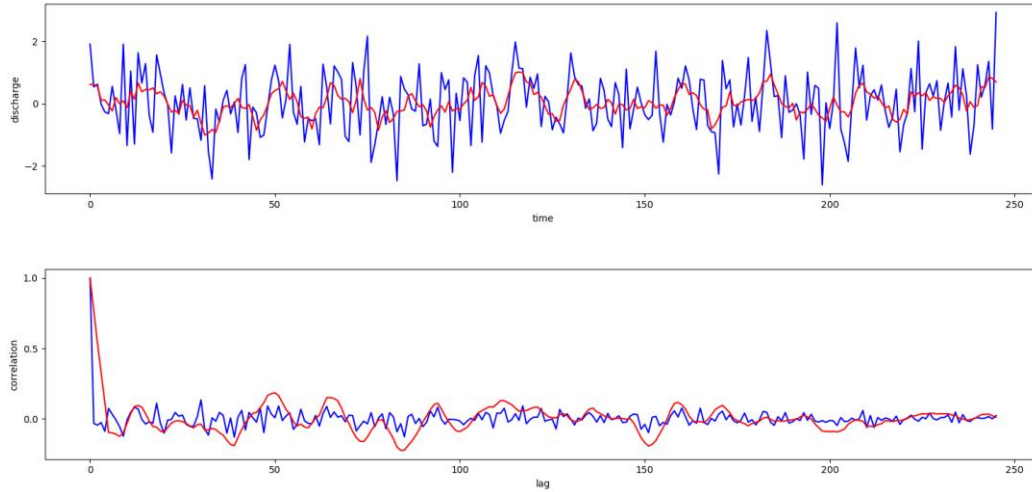


Figure 8: Autocorrelation diagrams

283 Understanding the correlation period between precipitation and spring response requires eliminating the
284 influence of the winter recharge period until the peak due to melting. Springs do not respond to winter and
285 spring precipitation; the water that arrives at springs depends on the melting process, which is correlated with
286 temperature fluctuations rather than precipitation.

287 Precipitation values were recorded by the Mascognaz meteorological station. The type of precipitation (solid
288 or liquid) was determined using the Parsivel 2 of the OTT, a modern laser disdrometer. The beginning of the
289 period selected for cross-correlation analysis was considered coincident with the beginning of the exhaustion
290 period; this was also true for the recession analysis using the Maillet and Boussinesq methods.

291 Comparing data from different years within the selected period revealed that the lag time between rainfall and
 292 discharge tended to be short. As shown in Fig. 9, the considered lag time was 3 days; analysing all years within
 293 the considered period resulted in a maximum value of 4 days and a minimum value of 1 (Tab. 5).

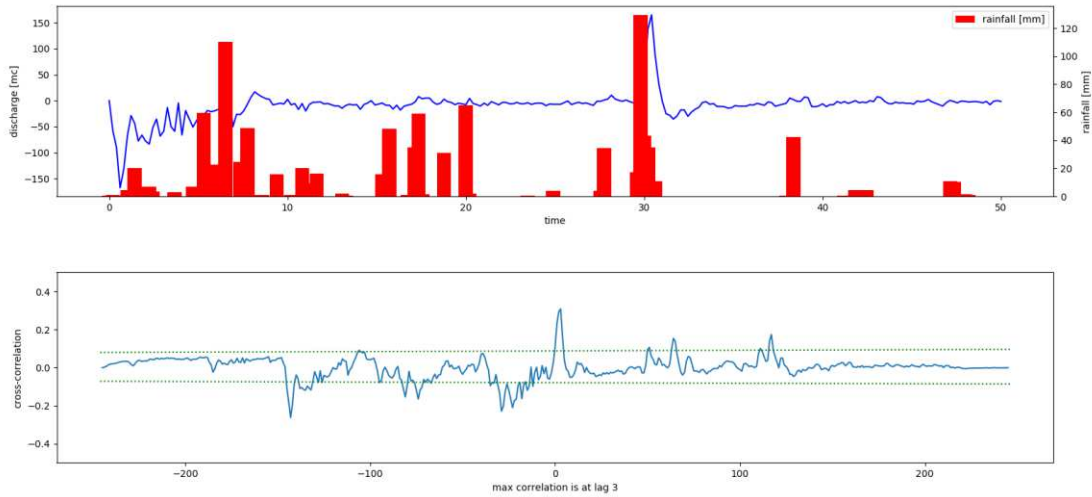


Figure 9: Cross correlation between rainfall and flow rate

Year	2011	2014	2015	2016
Cross correlation (lag time)	3	1	1	2

294 Table 5: Cross-correlation coefficient values obtained for the Mascognaz 1 spring

295 To verify the validity of the tool proposed and presented in this work, all of the results derived from the
 296 application were checked with manual calculations carried out by using Excel spreadsheets. By comparing the
 297 values obtained for the hydrodynamic parameters of the aquifer (α , W_0 and W_d) and the estimated indexes of
 298 vulnerability (V index) for all studied seasons, the proposed tool was found to be completely reliable.

299 5. Conclusions

300 New automated tools can potentially be applied to estimate aquifer hydrogeological parameters and monitor
 301 water spring behaviour. The effects of climate change on mountain springs can be intense, and tools are needed
 302 to guarantee a correct understanding of the dynamics of available resource exhaustion.

303 In this paper, SOURCE is an advanced semi-automatic Python tool that automates the hydrogeological
 304 characterisation of spring aquifers. This tool was tested through an analysis of the Mascognaz 1 mountain

305 springs. Graphical outputs, as well as hydrodynamic parameter values (e.g., VESPA index and auto- and cross-
306 correlation coefficients) for an aquifer, can be obtained from SOURCE. These graphs and values are crucial
307 for understanding the hydrogeological processes that characterise spring aquifers and for developing a proper
308 groundwater resource management strategy.

309 Unlike the software currently available through various university centres (e.g., RC software and the USGS
310 GW Toolbox), the proposed tool provides an accurate estimation of the vulnerability index and also provides
311 a recorded signal analysis using autocorrelation and cross-correlation statistical functions. A single software
312 package that contains all of the main methods of water spring analysis has the potential to significantly reduce
313 analysis times.

314 The SOURCE intuitive interface allowed not only researchers and hydrogeologists, but also non-expert users
315 to test the software and correctly use its functionalities for mountain springs analysis.

316 SOURCE is an open-source software tool, and the code is available for free download at
317 https://www.diati.polito.it/ricerca/aree/geologia_applicata_geografia_fisica_e_geomorfologia.

318 The authors are open to all comments and advice from users that could help to further implement the code and
319 improve the performances.

320 **Declarations**

321 **Funding**

322 Not applicable

323 **Conflicts of interest**

324 The authors declare that they have no known competing financial interests or personal relationships that
325 could have appeared to influence the work reported in this paper.

326 **Availability of data and material**

327 The hourly recorded data used to support the findings of this study have not been made directly available
328 because they are ownership of Politecnico di Torino. However, they are reported as graphs.

329 **Code availability**

330 The code is available for free download at

331 https://www.diati.polito.it/ricerca/aree/geologia_applicata_geografia_fisica_e_geomorfologia

332 **References**

- 333 Aller L, Bennet T, Lehr J H, Petty R J, Hackett G (1987). “DRASTIC: A Standardized System for Evaluating
334 Ground Water Pollution Potential Using Hydrogeologic Settings”. US EPA Report 600/287/035. U.S.
335 Environmental Protection Agency.
336
- 337 Amit H, Lyakhovsky V, Katz A, Starinsky A, Burg A (2002). Interpretation of spring recession curves. *Ground*
338 *Water* 40(5):543–551.
339
- 340 Angelini P (1997). Correlation and spectral analysis of two hydrogeological systems in Central Italy. *Hydrol.*
341 *Sci. J.* 42, 425–438. <https://doi.org/10.1080/02626669709492038>
342
- 343 Amanzio G, De Maio M, Suozzi E, Bertolo D, Lodi L P, Pitet L (2015). Global Warming in the Alps:
344 Vulnerability and Climatic Dependency of Alpine Springs in Italy. Regione Valle d’Aosta and
345 Switzerland, Canton Valais; G. Lollino et al. (eds.). *Engineering Geology for Society and Territory –*
346 *Volume 5*, DOI: 10.1007/978-3-319-09048-1_263. Springer International Publishing Switzerland 2015
347
- 348 Amanzio G, De Maio M, Suozzi E (2015). Vulnerability of Mountain Springs Affect by Climatic Change: A
349 New Method in a Porous Media Aquifer in Regione Automa Valle d’Aosta G. Lollino et al. (eds.).
350 *Engineering Geology for Society and Territory – Volume 5*, DOI: 10.1007/978-3-319-09048-1_259.
351 Springer International Publishing Switzerland 2015
352
- 353 Banzato C, Butera I, Revelli R, Vigna B (2017). Reliability of the VESPA index in identifying spring
354 vulnerability level. *J. Hydrol. Eng.* 22, 1–11. [https://doi.org/10.1061/\(ASCE\)HE.1943-5584.0001498](https://doi.org/10.1061/(ASCE)HE.1943-5584.0001498)
355
- 356 Barlow P M, Cunningham W L, Zhai T and Gray M (2017). U.S. Geological Survey Groundwater Toolbox
357 version 1.3.1, a graphical and mapping interface for analysis of hydrologic data: U.S. Geological Survey
358 Software Release, 26 May 2017, <http://dx.doi.org/10.5066/F7R78C9G>
359
- 360 Boussinesq J (1904). Recherches théoriques sur l’écoulement des nappes d’eau infiltrées dans le sol et sur le
361 débit des sources. *J. Math. Pure Appl.* 10:5–78
362
- 363 Cambi C, Dragoni W (2000). Groundwater yield, climatic changes and recharge variability: considerations
364 arising from the modelling of a spring in the Umbria-Marche Apennines. *Hydrogéologie*, n.4, ed. BRGM,
365 pp. 11-25.
366
- 367 Christe P, Amanzio G, Suozzi E, Mignot E, Ornstein P (2013). Global warming in the Alps: vulnerability and
368 climatic dependency of alpine springs in Italy, Regione Valle d’Aosta (Italy) and Canton Valais
369 (Switzerland). *Eur Geol–J Eur Fed Geol* 35:64–69 (ISSN:1028-267X)
370
- 371 Civita M, De Maio M (1997). Sintacs. Un sistema parametrico per la valutazione e la cartografia della
372 vulnerabilità degli acquiferi all’inquinamento. Metodologia e automatizzazione, Manuali di protezione
373 delle acque sotterranee. Pitagora
374
- 375 Dal Piaz G V (1992). Alpi dal Monte Bianco al Lago Maggiore. Guide geologiche regionali. Soc. Geol. It. BE-
376 MA ed., 3(2)
377
- 378 Dewandel B, Lachassagne P, Bakalowicz M, Weng P, Al-Malki A (2003). Evaluation of aquifer thickness by
379 analysing recession hydrographs. Application to the Oman ophiolite hard-rock aquifer. *J. Hydrol.* 274,

380 248–269. [https://doi.org/10.1016/S0022-1694\(02\)00418-3](https://doi.org/10.1016/S0022-1694(02)00418-3)
381
382 Fiorillo F, Esposito L, Guadagno F M (2007). Analyses and forecast of water resources in an ultra-centenarian
383 spring discharge series from Serino (southern Italy). *J Hydrol* 336:125–138
384
385 Fiorillo F (2014). The Recession of Spring Hydrographs, Focused on Karst Aquifers. *Water Resour. Manag.*
386 28, 1781–1805. <https://doi.org/10.1007/s11269-014-0597-z>
387
388 Fiorillo F, Doglioni A (2010). The relation between karst spring discharge and rainfall by cross-correlation
389 analysis (Campania, Southern Italy). *Hydrogeol. J.* 18, 1881–1895. [https://doi.org/10.1007/s10040-010-](https://doi.org/10.1007/s10040-010-0666-1)
390 0666-1
391
392 Foster S (1987). Fundamental Concepts in Aquifer Vulnerability, Pollution Risk and Protection Strategy:
393 International Conference, 1987, Noordwijk Aan Zee, the Netherlands Vulnerability of Soil and
394 Groundwater to Pollutants. Netherlands Organization for Applied Scientific Research, The Hague, 69-
395 86.
396
397 Galleani L, Vigna B, Banzato C, Lo Russo S (2011). Validation of a Vulnerability Estimator for Spring
398 Protection Areas: The VESPA index. *J. Hydrol.* 396, 233–245.
399 <https://doi.org/10.1016/j.jhydrol.2010.11.012>
400
401 Gattinoni P, Francani V (2010). Depletion Risk Assessment of the Nossana Spring (Bergamo, Italy) Based on
402 the Stochastic Modeling of Recharge. *Hydrogeol. J.* 18, 325–337. [https://doi.org/10.1007/s10040-009-](https://doi.org/10.1007/s10040-009-0530-3)
403 [0530-3](https://doi.org/10.1007/s10040-009-0530-3)
404
405 Gizzi M, Lo Russo S, Forno M G, Cerino Abdin E, Taddia G (2020). Geological and Hydrogeological
406 Characterization of Springs in a DSGSD Context (Rodoretto Valley – NW Italian Alps). *Appl. Geol.* 3–
407 19. https://doi.org/10.1007/978-3-030-43953-8_1
408
409 Gogu R, Dassargues A (2000). Current trends and future challenges in groundwater vulnerability assessment
410 using overlay and index methods. *Environ. Geol.* 39, 549–559. <https://doi.org/10.1007/s002540050466>
411
412 Imagawa C, Takeuchi J, Kawachi T, Chono S, Ishida K (2013). Statistical analyses and modeling approaches
413 to hydrodynamic characteristics in alluvial aquifer. *Hydrol. Process.*, 27, 4017–4027
414
415 Kova'cs A, Perrochet P, Kira'ly L, Jeannin P Y (2005). A quantitative method for the characterization of karst
416 aquifers based on spring hydrograph analysis. *Journal of Hydrology* 303, 152–164
417
418 Larocque M, Mangin A, Razack M, Banton O (1998). Contribution of correlation and spectral analyses to the
419 regional study of a large karst aquifer (Charente, France). *J. Hydrol.* 205, 217–231.
420 [https://doi.org/https://doi.org/10.1016/S0022-1694\(97\)00155-8](https://doi.org/https://doi.org/10.1016/S0022-1694(97)00155-8)
421
422 Lo Russo S, Amanzio G, Ghione R, De Maio M (2015). Recession hydrographs and time series analysis of
423 springs monitoring data: application on porous and shallow aquifers in mountain areas (Aosta Valley).
424 *Environ. Earth Sci.* 73, 7415–7434. <https://doi.org/10.1007/s12665-014-3916-z>
425
425 Maillet E (1905). *Essais d'hydraulique souterraine et fluviale*, Vol. 1. Herman et Cie, Paris, pp 218.
426
426 Middelkoop H, Daamen K, Gellens D, Grabs W, Kwadijk J C J, Lang H, Parmet B W A H, Schädler B, Schulla

- 427 J, Wilke K (2001). Impact of Climate Change on Hydrological Regimes and Water Resources
428 Management in the Rhine Basin. *Clim. Change* 49, 105–128. <https://doi.org/10.1023/A:1010784727448>
429
- 430 Panagopoulos G, Lambrakis N (2006). The contribution of time series analysis to the study of the
431 hydrodynamic characteristics of the karst systems: Application on two typical karst aquifers of Greece
432 (Trifilia, Almyros Crete). *J. Hydrol. - J. HYDROL* 329, 368–376.
433 <https://doi.org/10.1016/j.jhydrol.2006.02.023>
434
- 435 Reberski Lukac̃ J, Markovic´ T, Nakic´ Z (2013). Definition of the River Gacka springs subcatchment areas
436 on the basis of hydrogeological parameters. *Geologia Croatica* 66(1):39–53. doi:10.4154/gc. 2013.04
437
- 438 Tague C, Choate J, Grant G (2012). Parameterizing sub-surface drainage with geology to improve modeling
439 streamflow responses to climate in data limited environments. *Hydrol. Earth Syst. Sci. Discuss.* 9.
440 <https://doi.org/10.5194/hessd-9-8665-2012>

Figures

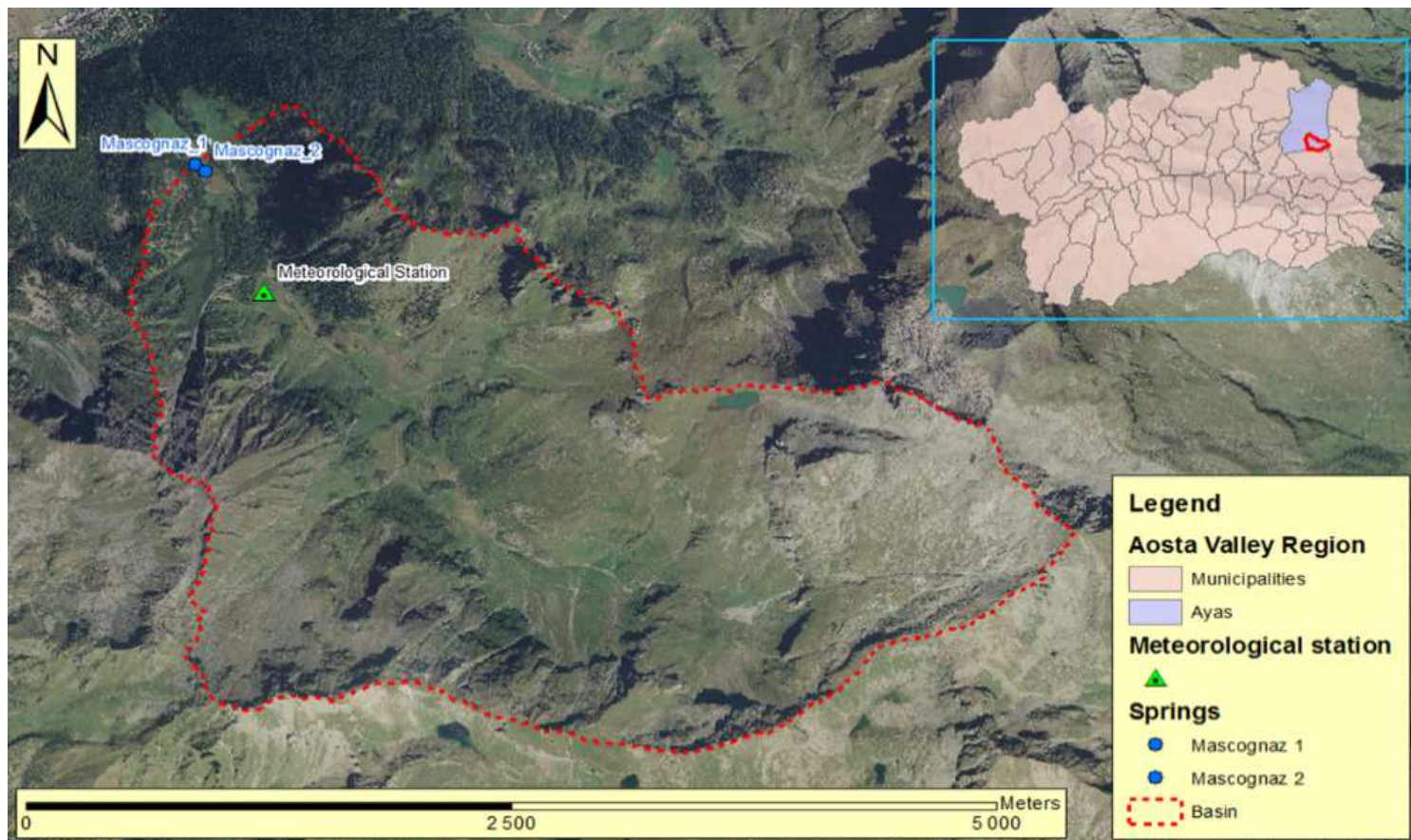


Figure 1

Mascognaz springs location Note: The designations employed and the presentation of the material on this map do not imply the expression of any opinion whatsoever on the part of Research Square concerning the legal status of any country, territory, city or area or of its authorities, or concerning the delimitation of its frontiers or boundaries. This map has been provided by the authors.



Figure 2

Overview of the instruments installed in the Mascognaz 1 spring



POLITECNICO DI TORINO

Tool developed by Politecnico di Torino 2020 thanks to the project INTERREG RESERVAQUA.

Water spring name

Filename

Date Start

Date Stop

Select type of Analysis All Recession curves Vespa Index Plot Data Cross Correlation

Select method for Recession curves: All Boussinesq None Maillet

For further informations contact:

Enrico Suozzi enrico.suozzi@polito.it

Martina Gizzi martina.gizzi@polito.it

Figure 3

GUI of the proposed Python tool

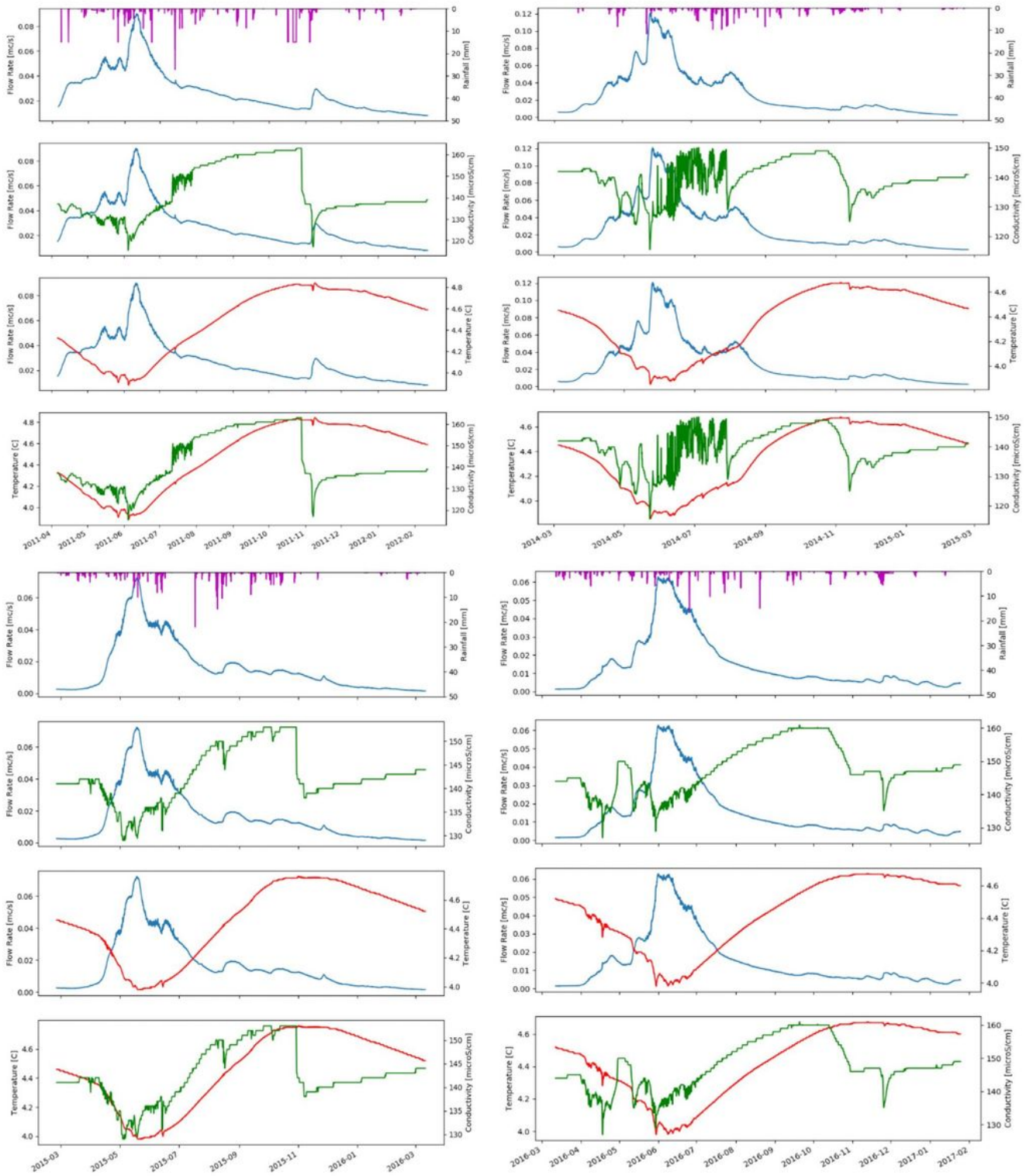
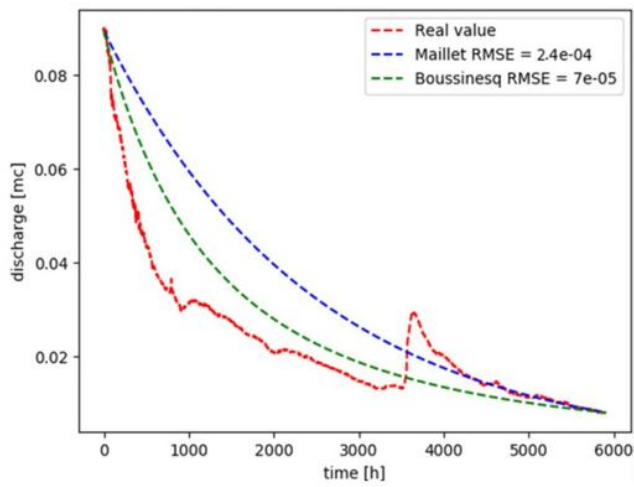
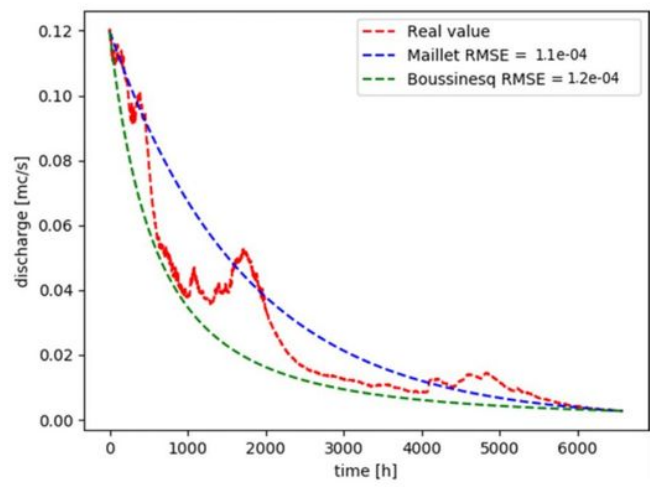


Figure 4

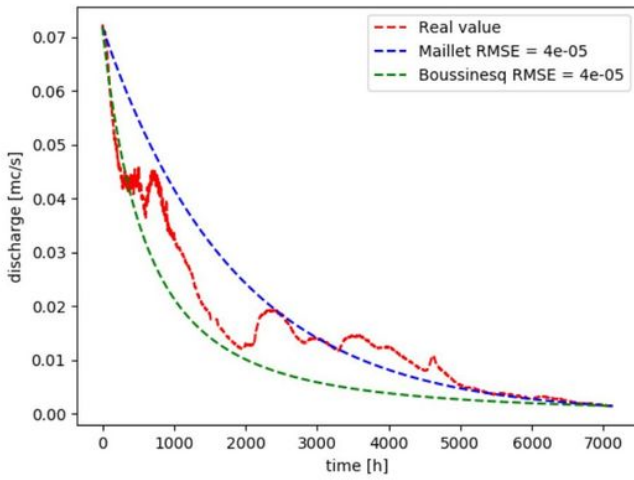
Mascognaz 1 spring hydrographs (NW Start 2011-04-06, Stop 2012-02-12; NE Start 2014-03-05 Stop 2015-02-24; SW Start 2015-02-25 Stop 2016-03-11; SE Start 2016-03-12 Stop 2017-01-25) for rainfall (violet lines), flow rate (blue lines), electrical conductivity (green lines) temperature (red lines)



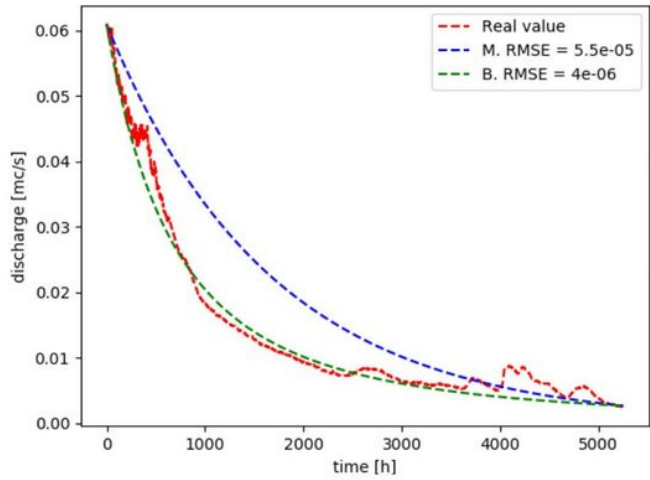
2011-2012



2014-2015



2015-2016



2017-2018

Figure 5

Mascognaz 1 recession curves based on the Boussinesq (1904) and Maillet (1905) methods

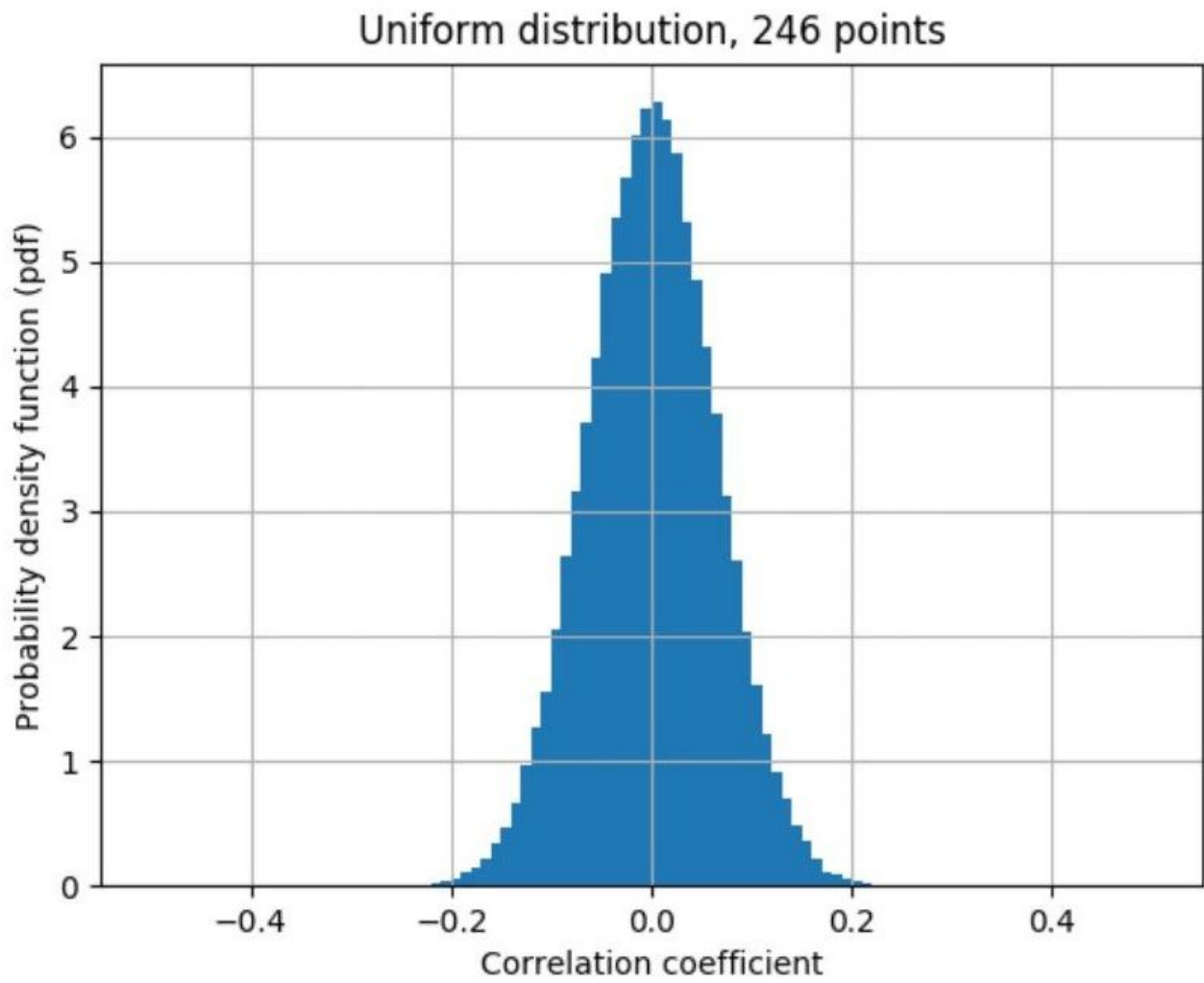


Figure 6

PDF of the estimated correlation coefficients (2011 dataset)

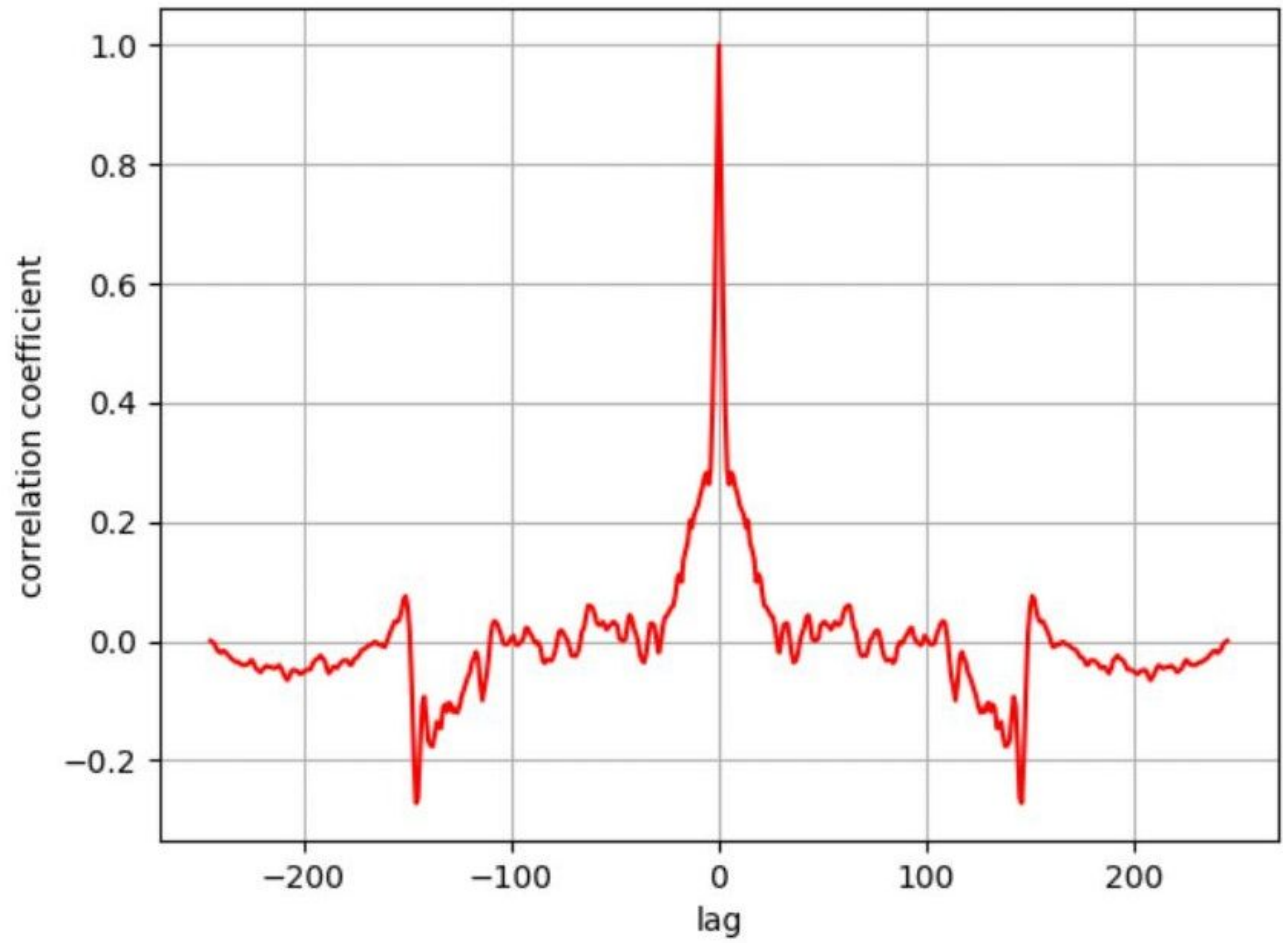


Figure 7

Estimated correlation coefficients, considering different time lags (2011 dataset)

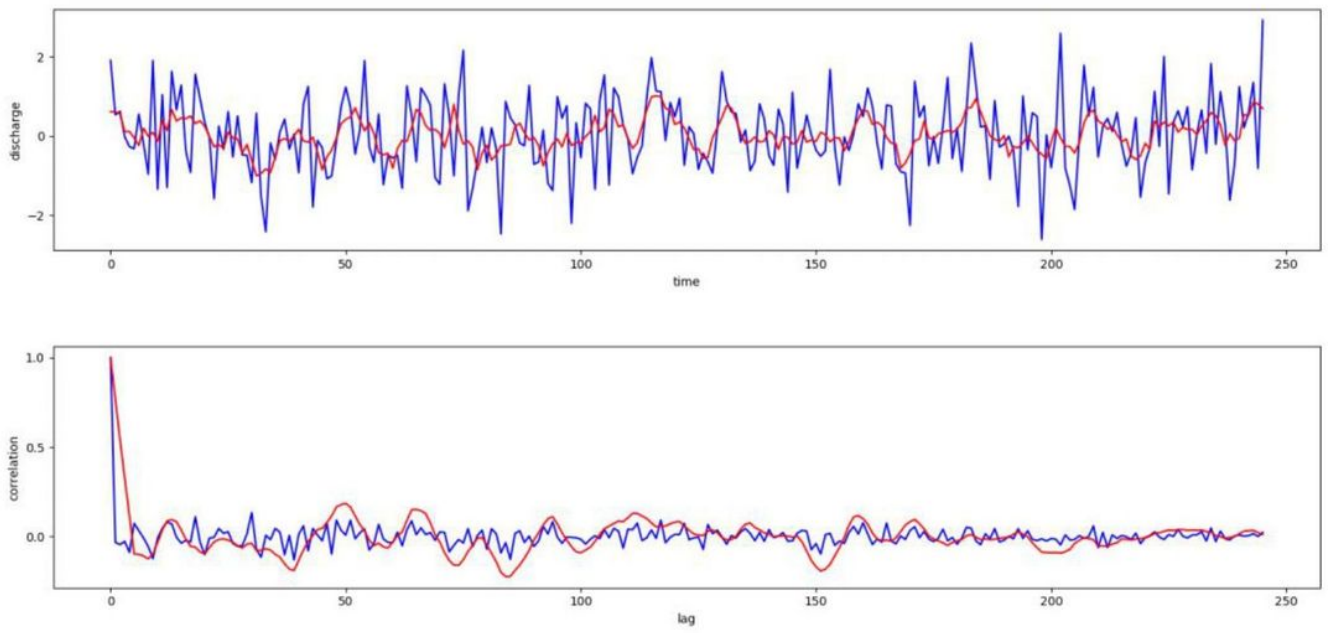


Figure 8

Autocorrelation diagrams

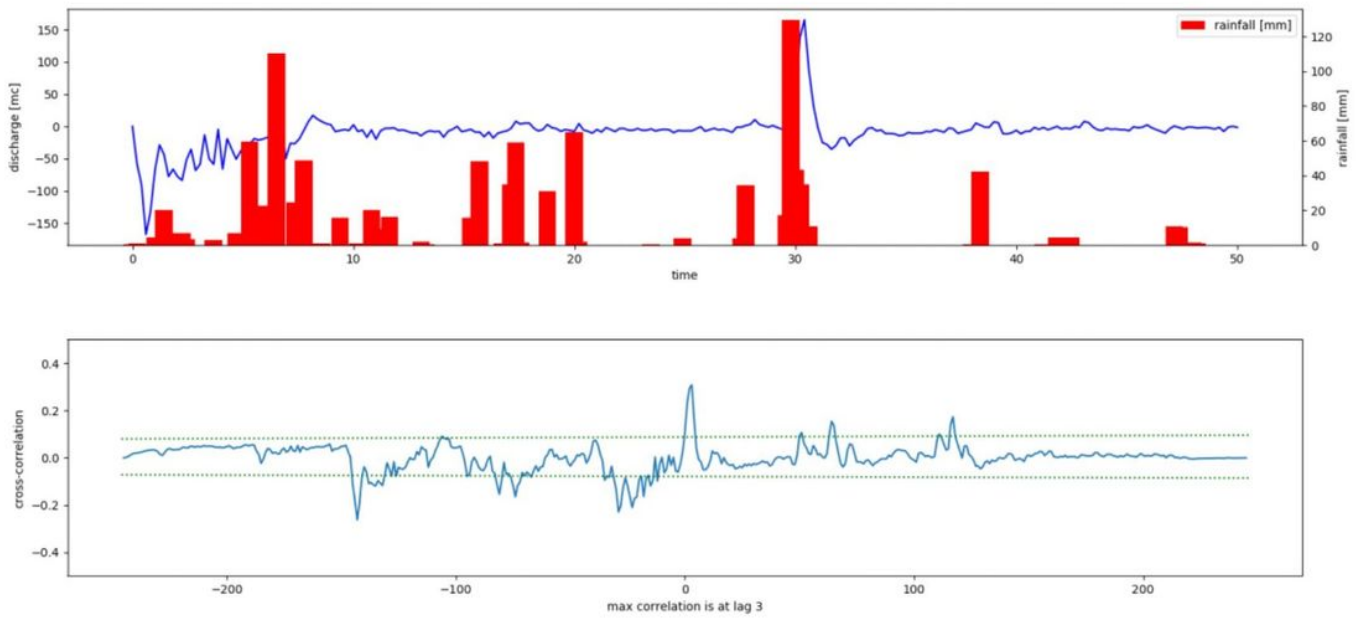


Figure 9

Cross correlation between rainfall and flow rate